ACTA ACUSTICA UNITED WITH ACUSTICA
Vol. 89 (2003) 980 – 991

Outdoor Sound Propagation: A Short Review on Analytical and Numerical Approaches

M. C. Bérengier, B. Gauvreau
Laboratoire Central des Ponts et Chaussées, Section Acoustique Routière et Urbaine, Centre de Nantes, Route de Bouaye, BP 4129, 44341 Bouguenais Cedex, France

Ph. Blanc-Benon, D. Juvé
Ecole Centrale de Lyon, Laboratoire de Mécanique des Fluides et d'Acoustique, Centre Acoustique 36, Avenue Guy de Collongue, 69134 Ecully Cedex, France

Summary
Prediction of sound pressure levels at medium and large distances from road, railway and industrial sources, has been of considerable interest in environmental acoustics for several years. At the beginning, the fundamental hypotheses were very simplified: homogeneous and isotropic propagation medium with perfectly reflecting grounds. Then, during the following years, various parameters were successively taken into account. In that way, different sound propagation effects in the vicinity of absorbing or mixed grounds, with or without barriers, fluctuating atmospheric conditions with or without turbulence were considered. In a first approach, all these works were based on analytical methods (Ray tracing technique, Geometrical Theory of Diffraction, Creeping wave theory, etc.). In the recent years, new numerical methods were investigated (Parabolic Equation approach, Finite and Boundary Element Techniques, etc.). These different methods have been highlighted through adapted softwares able to predict sound pressure levels for a rather large number of situations. These computing codes, indexed as research and/or commercial softwares have been highly validated. In spite of the increasing improvements of the theoretical modelling and resolution methods, which became possible due to the new computing technologies, progresses are still possible. This paper deals with analytical and numerical approaches, pointing out in particular their respective validity domains.

PACS no. 43.28.J

1. Introduction

Propagation phenomena of sound waves in the environment are very complex and a large number of parameters have to be considered. The main ones are related to the physical characteristics of the propagation medium (air) on one hand, and to the boundary conditions (natural or artificial grounds, barriers, etc.) on the other hand. Thus, the modelling process requires consideration of many different mechanisms such as: the geometrical spreading, the molecular absorption, reflection processes on the limiting surfaces, various diffraction effects, the influence of the temperature and wind speed profiles and finally, the influence of the atmospheric turbulence.

Depending on the complexity of the problem to be treated, different approaches can be considered. During the last thirty years, various authors [1] worked on this important problem by successive steps integrating at each step a new parameter. In the next sections, we successively discuss about different analytical and numerical models allowing taking into account a large number of realistic situations.

Received 15 February 2002,
accepted 19 February 2003.

2. Analytical approaches

2.1. Ground effects on the sound wave propagation

Independently of the ground type and composition between the source and the receiver: homogeneous or mixed, their respective influence on the sound wave attenuation along the propagation path is important. This attenuation is frequency dependent and function of the incidence angle and propagation distance. More grazing is the incidence and higher is the frequency, stronger is the attenuation. This general principle can be largely applied to natural absorbing grounds. Therefore, it is not equivalent for certain porous structures with a rigid internal skeleton such as pervious road surfaces. In that case, particular phenomena related to the surface wave can induce sound level amplifications for frequencies above 1 kHz and angles of incidence greater than 10 degrees [2, 3].

At the beginning, the authors only considered a homogeneous and isotropic atmosphere in which the vertical sound speed gradient $\partial c/\partial z$ was equal to zero.

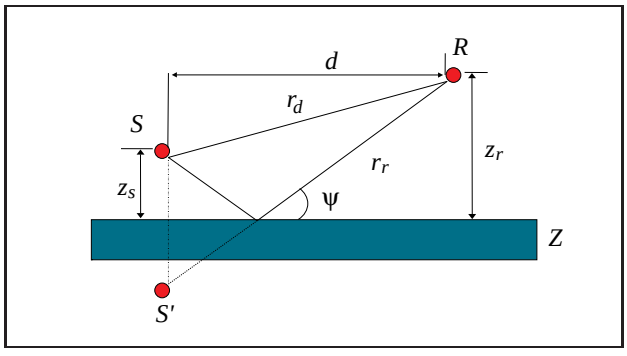

Figure 1. Homogeneous ground: geometry of the problem.

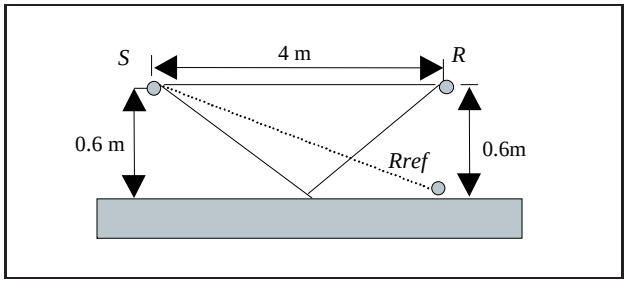

Figure 2. First validation: geometrical set-up.

2.1.1. Propagation above a homogeneous ground

In order to solve this problem, several approaches based on the ray tracing theory have been investigated [1]. Two of them are particularly used: the one introduced by Rudnick [4], further developed by Donato [5], Chessell [6] and Embleton *et al.* [7, 8] and finally, the one developed by Thomasson [9, 10]. In those approaches, the sound field is split into three terms: a direct wave between the source and the receiver, a reflected wave on the ground and a surface wave.

Other approaches have also to be mentioned. They use the layer potentials representation and have been developed by P. Filippi and D. Habault [11, 12].

In the case of an omnidirectional point source above an absorbing plane characterised by its normalized surface impedance $Z(f) = \zeta(f)/\rho c$ (ζ and ρc respectively represent the characteristic impedance of the ground and the impedance of air), the sound pressure level at the receiving point R can be approached through the equation:

$$\frac{p}{p_0} = \frac{A_d}{r_d}\mathrm{e}^{\mathrm{i}kr_d} + Q\frac{A_r}{r_r}\mathrm{e}^{\mathrm{i}kr_r}. \tag{1}$$

The spherical reflection coefficient Q is given by the following expression:

$$Q = R_p + (1 - R_p)F(w). \tag{2}$$

$k = \omega/c$ is the wave number in the air where ω is $2\pi f$. f is the frequency and c the sound celerity. A_d and A_r are the magnitudes of the direct and reflected waves. R_p is the plane wave reflection coefficient,

$$R_p = \frac{Z\sin\psi - \chi}{Z\sin\psi + \chi}, \tag{3}$$

and $F(w)$ an asymptotic development given by:

$$F(w) = 1 + \mathrm{i}\sqrt{\pi}w\exp(-w^2)\mathrm{erfc}(-\mathrm{i}w), \tag{4}$$

where

$$w^2 = 2\mathrm{i}kr_r\chi^2\frac{1}{Z(1-R_p)^2} \tag{5}$$

and

$$\chi = \sqrt{1 - \left(\frac{k}{\kappa}\right)^2\cos^2\psi}. \tag{6}$$

κ is the complex wave number inside the porous structure and ψ the incidence angle. All the variables of the problem are calculated with a $\mathrm{e}^{-\mathrm{i}\omega t}$ time dependence.

According to the ground composition, various impedance models can be used. For natural grounds or for reflecting road surfaces, the Delany and Bazley model [13] is the most commonly used. It only considers one parameter which is the airflow resistivity σ, in kN s m^{-4}.

For the porous road surfaces, well-adapted models exist. Two approaches have been tested and compared [2]: A phenomenological one jointly developed by J. F. Hamet and M. Bérengier [14] and a microstructural one developed in the same time by K. Attenborough [15] and by Y. Champoux [16]. These models require several parameters such as the airflow resistivity σ in kN s m^{-4}, the open porosity Ω and one or several shape factors representative of the medium tortuosity (q^2), the viscous and thermal dependences, respectively s_p and s_k.

According to these hypotheses, in many situations, the sound energy above a plane characterised by its normalized impedance Z can be expressed by the equation

$$\begin{aligned}\langle p\rangle \;=\; & \frac{[A_d]^2}{r_d^2} + |Q|^2\frac{[A_r]^2}{r_r^2} \\ & + \frac{2|Q|A_dA_r}{r_dr_r}\cos\left[\omega(\tau_r - \tau_d) + \mathrm{Arg}(Q)\right],\end{aligned} \tag{7}$$

where $\tau_{r,d} = r_{r,d}/c$.

Equation (7) can also be used to calculate the sound attenuation between two receivers located at different heights above the ground (cf. Figure 2). This corresponds to the results presented on Figure 3, for a short propagating distance (4 m). For this comparison between experiment and prediction, the sound pressure levels were obtained using an impulse method described in [17] with the sound source located 0.60 m above the ground and the two receivers respectively on the ground and 0.60 m above de ground surface

A nice agreement between prediction and measurement is found. Nevertheless, we have to keep in mind that it is

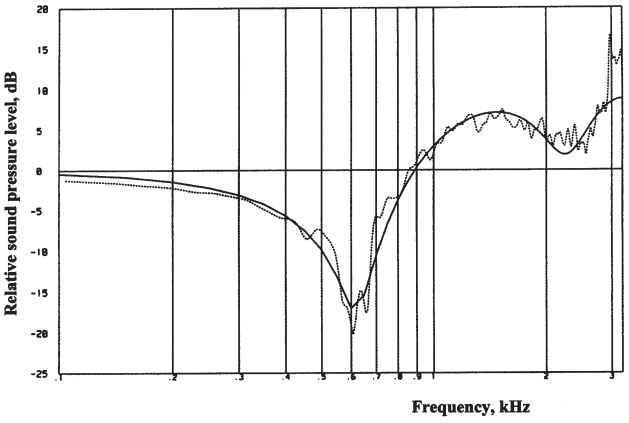

Figure 3. Relative sound pressure level versus frequency for a homogeneous ground $z_S = z_{R1} = 0.60\,\mathrm{m}$; $z_{R2} = 0.006\,\mathrm{m}$; $d = 4\,\mathrm{m}$; Grassy ground ($\sigma = 160\,\mathrm{kN\,s\,m^{-4}}$). (——): prediction; (– – –): measurement.

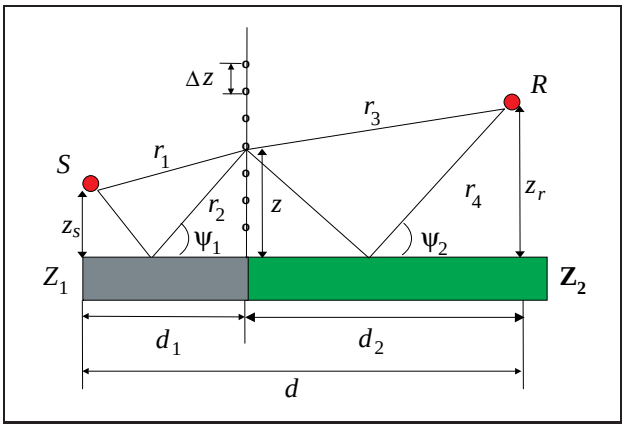

Figure 4. Mixed ground: geometry of the problem.

an ideal situation, which does not really fit with real conditions. In fact, we are very often in presence of irregular surfaces, mixed grounds presenting impedance discontinuities, large propagation distances and mainly, inhomogeneous and fluctuating atmospheric conditions. In order to solve these various situations, several predicting models are available. They will be detailed in the next section.

2.1.2. Propagation above a mixed ground

Sound propagation modelling above homogeneous ground is interesting but not sufficient for a large number of situations, and mainly when traffic noise is concerned. In fact, the sound source, which is in the close vicinity of the road surface, generates a wave that propagates across a discontinuity. Apart the case of porous pavements, two different media have to be taken into account: a totally reflecting road surface and an absorbing natural ground (Figure 4).

Identically to the homogeneous grounds, several approaches can be considered. One of the most adapted to this problem has been developed by K.B Rasmussen [18]. It is based on a Green formulation. In spite of the excessive computing time, this method is nevertheless more accurate than semi-empirical formulations [19, 20], and particularly, for grazing incidence where source and receiver are very close to the ground (Figure 5).

The Kirchhoff-Huygens formulation implemented by Rasmussen is limited to an integration in the vertical plane above the impedance jump. Using the stationary phase technique, the formulation can be expressed by a single integral easy to compute (equation 8).

$$p(\omega) = \sqrt{8\pi k}\, d_2 \frac{\mathrm{e}^{-\mathrm{i}\pi/4}}{16\pi^2} I, \tag{8}$$

with

$$I = \int_0^\infty \left[p_1 + Q_2 p_2 + Q_1 p_3 + Q_1 Q_2 p_4\right] \mathrm{d}z, \tag{9}$$

where Q_1 and Q_2 are the spherical reflection coefficients related to the two grounds characterised by their normalized impedances Z_1 and Z_2 respectively. The different terms p_i ($i = 1, 4$) correspond to the acoustic energy transmitted along the rays r_i ($i = 1, 4$). From a numerical point of view, the integral is calculated through the trapeze method (equation 10).

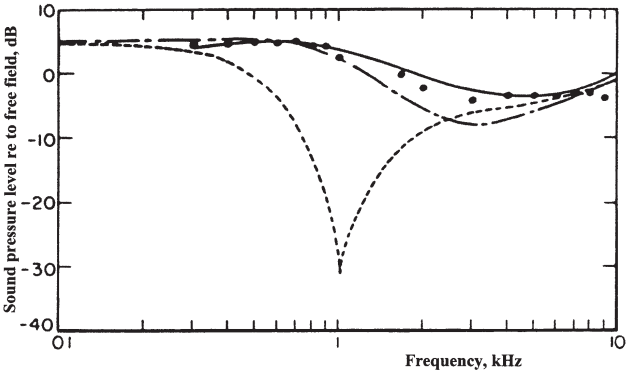

Figure 5. Sound pressure level relative to free field above a mixed ground: comparison between measurement: (• • •) and prediction: (——): [18]; (– – –): [19]; (– - –): [20] $z_S = 0.01\,\mathrm{m}$; $z_R = 0.02\,\mathrm{m}$; $d = 2.4\,\mathrm{m}$; $d_1 = 2.2\,\mathrm{m}$; $\sigma_1 = 20000\,\mathrm{kN\,s\,m^{-4}}$; $\sigma_2 = 50\,\mathrm{kN\,s\,m^{-4}}$.

$$I = \sum_n \left[p_1 + Q_2 p_2 + Q_1 p_3 + Q_1 Q_2 p_4\right] \Delta z. \tag{10}$$

Therefore, this technique requires a Δz sufficiently small and n sufficiently large to insure a good convergence. In practice, the integration cannot be performed from $z = 0$ and $z = \infty$ but has to be stopped at a height $z_{\max} \leq \infty$. The choice for Δz and $z_{\max}$ is a compromise between sufficient convergence and computing time. In addition, these two parameters are frequency dependent. Rasmussen [18] details the various limitations for low and high frequencies. It has to be mentioned also that for extreme configurations, convergence is not achieved at frequencies below 300 Hz.

2.2. Effect of the atmospheric conditions on the sound propagation

After several years dedicated to researches on the influence of ground effects on outdoor sound propagation (with and without impedance discontinuity), in homogeneous media ($\partial c/\partial z = 0$), important works have been developed to consider the meteorological effects in theoretical models. Thus, followed many in situ experiments, which underlined large variations of the sound pressure levels (up to 20 dBA) for opposite meteorological conditions [21]: for instance, the negative refraction ($\partial c/\partial z < 0$) and the positive refraction ($\partial c/\partial z > 0$). In a first approximation, linear sound speed profiles were considered ($c(z) = c_0(1 + az)$). With this hypothesis, sound ray paths are circular. Afterwards, mixed grounds were introduced [22, 23].

2.2.1. Propagation for a negative refraction condition

Those conditions can be observed during a very sunny day or for an upwind situation. In that case, a negative vertical sound velocity gradient appears and influences the sound ray paths that are curved upwards, producing an acoustic shadow region (Figure 6).

Our modelling approach is based upon the creeping wave theory. In the vicinity and inside the shadow zone, the sound field produced by a point source of magnitude $\hat{S}$ is obtained after resolution of a partial derivative equation system (wave equation + boundary conditions) through a bi-dimensional Fourier transform [24] (Equation 11).

$$p(d,z) = -\hat{S}\int_{-\infty}^{+\infty} H_0^{(1)}(kd)P(z,k)k\,\mathrm{d}k. \qquad (11)$$

Inside the refraction zone, if $d > z_s + z$ or $z = z_r$ (receiver height), after calculation of the integral by the residue method, the following expression of the acoustic pressure is finally obtained:

$$p(d,z) = \frac{\pi}{\lambda}\mathrm{e}^{\mathrm{i}\pi/6}\hat{S}\sum_n H_0^{(1)}(k_n d) \frac{Ai\left(b_n - \frac{z_s}{\lambda}\mathrm{e}^{2\mathrm{i}\pi/3}\right) Ai\left(b_n - \frac{z_s}{\lambda}\mathrm{e}^{2\mathrm{i}\pi/3}\right)}{[Ai'(b_n)]^2 - b_n[Ai(b_n)]^2}, \qquad (12)$$

where $b_n = \tau\mathrm{e}^{2\mathrm{i}\pi/3} = (k_n^2 - k_0^2)\lambda^2\mathrm{e}^{2\mathrm{i}\pi/3}$ are the zeroes of the equation $Ai'(b_n) + q\mathrm{e}^{\mathrm{i}\pi/3}Ai(b_n) = 0$. $H_0^{(1)}$ is the Hankel function of the first kind and of order 0.

If a sufficient number of terms in the series are considered, the expression of $p(d,z)$ is also valid above the limiting ray. In that case, this solution is more satisfactory than this given by Pierce [24], which is limited to the shadow zone. This solution can be simplified when $Z \to \infty$.

When the receiver is deeply located in the shadow region, the acoustic field is given by the first term of the series, which represents the less attenuated propagative mode. In the other situations, approximations can be eventually considered by expressing the Hankel and Airy functions in the sound field formulation by their asymptotic assumptions.

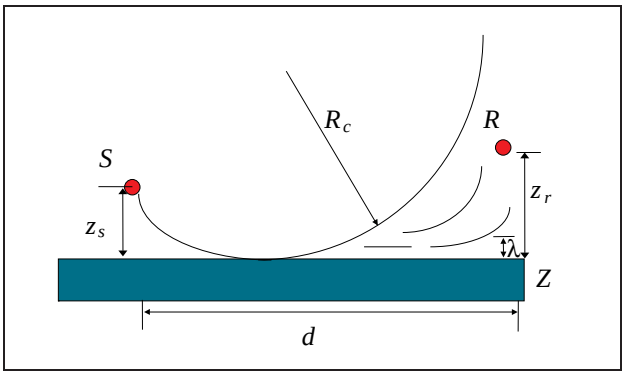

Figure 6. Negative refraction condition above a homogeneous ground: geometry of the problem.

For the most general situations, the number of terms of the series can be important ($10 < n < 50$). It mainly depends on the respective locations of the source and receiver with respect to the limiting ray. To model the propagation of the electromagnetic and radio waves over large distances between stations on the Earth and several ships situated in various locations on the ocean, Hill, Wait and Jones already used this theoretical approach [25, 26].

Above the limiting ray (illuminated zone), this method gives comparable results to the geometrical approach. This last one assumes that an analogy between the propagation above a plane surface in a stratified atmosphere and propagation above a curved surface in a homogeneous atmosphere exists. Different theoretical predictions have been compared to experiments on scale model (above a curved surface) as well as on real sites [22].

Formulations developed for a homogeneous ground have been afterwards extended to mixed grounds, for instance, a road surface and its close environment. In that case, the sound pressure is

$$p(Z_1,Z_2) = p_1(Z_1)\,D\,p_2(Z_2), \qquad (13)$$

with $D = D_1^{\alpha}D_2^{1-\alpha}$, where $\alpha = d_2/d_1$, $d_1 = d(S,S')$ and $d_2 = d(S',R)$.

S' is a fictitious sound source located just above the impedance discontinuity at a height $z_{S'}$.

$$D_1 = \frac{p(Z_1)}{p_1(Z_1)p_2(Z_1)}$$

and

$$D_2 = \frac{p(Z_2)}{p_2(Z_1)p_1(Z_2)}. \qquad (14)$$

$p(Z_1)$ and $p_i(Z_1)$ are developed in terms of creeping waves as detailed in [22].

Figure 7 shows the difference between the propagation in a shadow zone (equation 13) and in a homogeneous medium (equation 8) when the sound source is located above a reflecting road surface and the receiver above an absorbing grassy ground. The upper and lower dotted lines respectively correspond to an equivalent homogeneous hard ground ($\sigma_1 = 20000\,\mathrm{kN\,s\,m^{-4}}$) and soft ground ($\sigma_2 = 200\,\mathrm{kN\,s\,m^{-4}}$). At large distances, the ex-

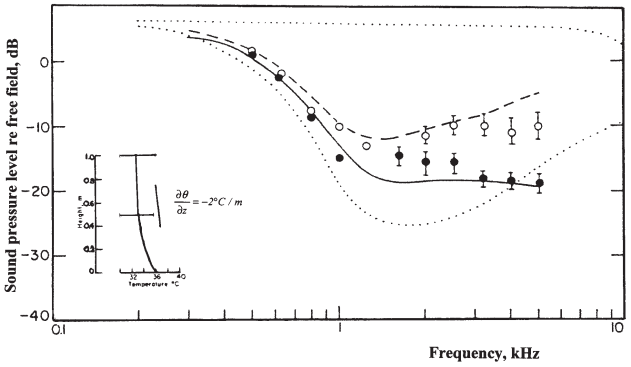

Figure 7. Negative refraction condition: comparison between (● ● ●, ○ ○ ○): measurements, (——): equation (13); (– – –): equation (8); · · ·: homogeneous grounds; $z_S = 0.08$ m; $z_R = 0.25$ m; $d = 25.8$ m; $d_1 = 5.8\,m$, $\sigma_1 = 20000$ kN s m^{-4}, $\sigma_2 = 200$ kN s m^{-4}.

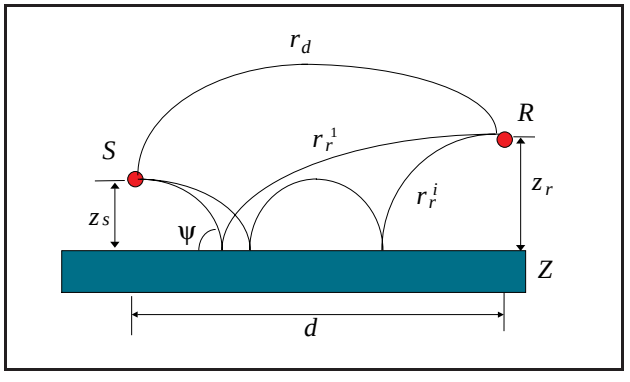

Figure 8. Positive refraction condition above a homogeneous ground: Geometry of the problem.

cess attenuations in the shadow zone can be very important, and often unrealistic with respect to measured relative sound pressure levels. This is mainly due to the turbulence effects, which have not been introduced in this formulation. Nevertheless, these effects have been considered in the numerical approaches detailed in section 3.

2.2.2. Propagation for a positive refraction condition

In that case, the sound rays are curved downwards. Thus, they are reflected one or several times on the ground (Figure 8).

The number of reflections depends in the same time on the respective source and receiver heights and the propagation distance. The sound ray curvature is due to the influence of a positive vertical sound speed gradient. Such situations can be observed during thermal inversions and, for downwind conditions. For particular geometric configurations, different authors [27, 28] have already investigated theoretical modelling of such propagating conditions. More recently, this has been improved in order to take into account more realistic situations [29].

As an example, those results have been widely used for the elaboration of the New French Traffic Noise Predicting Method [30], currently standardised under the reference XP S 31-133 [31].

The modelling technique is also based on the geometrical acoustic theory. After resolution of a 4th order equation, the abscissas of the reflecting points on the surface are determined. Thus, the number of bounces N can also be evaluated (equation 15). Afterwards, it is necessary to calculate the different lengths of the curved sound paths and the respective propagation delays.

A similar formulation of equation (7), which considers all the acoustic paths between the source and the receiver, allows calculating the global expression of the sound pressure level. It corresponds to the sum of the contribution of each acoustic path issued from the source and reaching the receiver (equation 16).

$$n(n+1)x^4 - (2n+1)dx^3 + \left[b_r^2 + (2n^2-1)b_s^2 + d^2\right]x^2 - (2n-1)b_s^2 dx + n(n-1)b_s^4 = 0, \qquad (15)$$

$$p^2 = \sum_{i=1}^{N} \frac{A_i^2 |Q_i|^2}{r_i^2} + 2\sum_{i=2}^{N}\sum_{j=1}^{i-1} \frac{A_i |Q_i| A_j |Q_j|}{r_i r_j} \cdot \cos\left[\omega(\tau_j - \tau_i) + \mathrm{Arg}\left(\frac{Q_j}{Q_i}\right)\right], \qquad (16)$$

where A_i represents the atmospheric absorption calculated from the ISO standard 9613-1 [32]. r_i and τ_i respectively represent the sound ray paths and the time delays. At the first iteration, ($r_1 = r_d$), the spherical reflection coefficient Q_1 is set to unity. For the reflected paths ($r_{i(i>1)} = r_r^i$), Q is expressed by the equation already mentioned in section 2.1.1. In the case of multi-reflections, each sound ray is reflected $i-1$ times between the source and the receiver. Thus, the sound pressure associated to this path is weighed by a coefficient Q_i function of the angle of reflection ψ_i and, the order of reflections $Q_i = [Q(\psi_i)]^{n_i}$. When N is equal to 2 (1 direct ray + 1 reflected ray), the equation proposed by Hidaka [27] is obtained.

r_i and τ_i have the following expressions

$$r_i = r(z_s) + r(z_r) + 2(n-1)r(z_m), \qquad (17)$$

$$\tau_i = \tau(z_s) + \tau(z_r) + 2(n-1)\tau(z_m), \qquad (18)$$

where $r(z_s)$ and $\tau(z_s)$ represent the path length and the time delay between the source and the first reflection, $r(z_r)$ and $\tau(z_r)$ the path length and the time delay between the source and the last reflection and the receiver and $2r(z_m)$ and $2\tau(z_m)$ the path length and the time delay between two successive reflections. General formulations for r and τ are detailed in [28]. When the values of the vertical sound speed gradient are small or when the source-receiver distances are relatively short (less than 200 metres), only one reflection occurs. In the other situations, N reflections will be considered.

Afterwards, turbulence effects have been taken into account by adding to the magnitude terms and to the wavenumber $k = \omega/c$ a fluctuating term whose random component is normally distributed [33]. In that case, we write $A_1 = 1 + a_1$, $A_{i(i>1)} = 1 + a_i$, $k_1 r_1 = kr_1 + \delta_1$ and $k_i r_i = kr_i + \delta_i$ for $i > 1$. a_1, a_i, δ_1 and δ_i are Gaussian variables with $\langle a_1^2 \rangle$, $\langle a_i^2 \rangle$, σ_1 and σ_i as respective standard

Table I. Comparison between measurement and prediction on the site of La Crau (France); $z_S = 6$ m; $\sigma = 300$ kNsm^{-4}.

Distance S/R (m)	Receiver height (m)	Measurement (dBA)	Prediction (dBA)
160	6.0	0 ± 1.1	0.1
	1.5	2.5 ± 1.5	-0.1
320	6.0	-0.3 ± 1.4	-0.4
	1.5	4.6 ± 1.4	4.2
640	6.0	3.7 ± 2.7	2.5
	1.5	8.5 ± 2.8	8.3

deviations. The main parameters connected to the turbulence are the intensity $\langle \mu^2 \rangle$ and the scale L. For typical situations representative of traffic noise, $\langle \mu^2 \rangle$ values are inside the range $[2 \cdot 10^{-6}; 20 \cdot 10^{-6}]$ and L close to 1 [33]. The mean value of the sound pressure level is then:

$$\langle p^2 \rangle = \sum_{i=1}^{N} \frac{A_i^2 |Q_i|^2}{r_i^2} + 2 \sum_{i=2}^{N} \sum_{j=1}^{i-1} \frac{A_i |Q_i| A_j |Q_j|}{r_i r_j} \cdot \cos\left[\omega(\tau_j - \tau_i) + \mathrm{Arg}\left(\frac{Q_j}{Q_i}\right)\right] \mathrm{e}^{-\sigma_1^2 (2 - \rho_i - \rho_j)}. \quad (19)$$

Equation (19) assumes that $\langle a_1^2 \rangle = \langle a_i^2 \rangle = \langle a^2 \rangle$. In that case, $A_1 = 1 + \langle a^2 \rangle$ and $A_{i,j} = 1 + \langle a^2 \rangle \phi_{i,j}$, where $\rho_{i,j}$ and $\phi_{i,j}$ are the magnitude and phase covariances.

In contrary to the situation with a negative refraction condition for which the influence of turbulence on the sound pressure level can reach several decibels [33], for positive refraction conditions, it only represents a few decibels. This can be justified by arguing that the sound pressure level is already high due to the large number of acoustic rays, which arrive to the receiver.

The values detailed in Table I show the validity of the prediction for a propagation on a flat ground for a large distance (640 m) and for to different receiver heights. These values (averages and standard deviations) correspond to the difference between the homogeneous condition ($\partial c / \partial z = 0$) and the positive refraction condition ($\partial c / \partial z > 0$).

3. Numerical approaches

During the last decade, propagation of sound above plane and heterogeneous grounds, including or not meteorological effects, has been extensively studied analytically, numerically and/or experimentally. Different numerical approaches such as Fast-Field Program without [34] and with turbulence [35], Boundary Element Methods [36, 37, 38, 39] and more recently, Meteo-BEM [40] have been successfully compared to analytical solutions and experiments for several usual situations. Nevertheless, when considering complex environments, mixed influence of terrain topography and atmospheric conditions has to be taken into account. In those particular situations where the propagation medium is not stationary with creation of mean motion or velocity fluctuations, numerical approaches based on parabolic equations seem to be well adapted to the problem. Different methods of resolution have been investigated. The main ones are: the Split-Step Fourier Method [41], the Crank-Nicholson scheme (CN-PE) [42, 43], the Green Function Parabolic Equation (GF-PE) [44, 45], the Generalized Terrain Parabolic Equation (GT-PE) [46], the Mean-Wind and Turbulent-Wind Wide-Angle Parabolic Equation (MW-WAPE, TW-WAPE) [47, 48]. Amongst these techniques, a mixed method called "Split-Step Padé" has been validated [49, 50]. It appeared to be reliable with respect to its obvious advantages in terms of angular aperture, CPU time and its capability to consider the main phenomena: from flat and homogeneous grounds to complex situations including mixed and/or non flat grounds.

Presently, some limitations of the PE models concern: the consideration of the back-scattered energy, the integration of the 3D effects and the wind characteristics in the equation. Further investigations on these aspects are currently in progress [51].

3.1. The parabolic equation

In the approximation of linear acoustics, the sound pressure level is solution of the elliptic Helmholtz equation. Following the hypothesis of an azimuthal symmetry of the acoustic field, this equation can be expressed in 2D:

$$\left(\frac{\partial^2}{\partial r^2} + \frac{1}{r}\frac{\partial}{\partial r} + \frac{\partial^2}{\partial z^2} + k^2\right) p = 0, \quad (20)$$

where r and z are the horizontal and vertical coordinates respectively and $k = k_0 n(r, z)$. n is the refraction index and k_0 a reference wave number.

The acoustic pressure is then split into two components: a propagating cylindrical wave, represented by the Hankel function and its assumption in the far field ($k_0 r \gg 1$), and an envelope function $u(r, z)$, which is slowly range dependent:

$$p(r, z) = u(r, z) H_0^{(1)}(k_0 r) \approx \frac{1}{\sqrt{r}} u(r, z) \exp(\mathrm{i} k_0 r). \quad (21)$$

If we assume that the range dependence of the refraction index $n(r, z)$ is weak and, that the backscattering acoustic energy is negligible, $u(r, z)$ evolution is then governed by the unidirectional parabolic equation:

$$\frac{\partial u(r, z)}{\partial r} = \mathrm{i}(\sqrt{\mathcal{P}} - 1) u(r, z), \quad (22)$$

where the pseudo-differential operator $\sqrt{\mathcal{P}}$ is defined by:

$$\mathcal{P} = \frac{\partial^2}{\partial z^2} + k_0^2 n^2. \quad (23)$$

According to the $\sqrt{\mathcal{P}}$ series development, various approximations lead to different angle limitations for the sound propagation and different numerical schemes.

3.2. The Split-Step Padé method

A new pseudo-differential operator $\mathcal{P}'$ is defined by $\mathcal{P}' = 1 + \xi + \eta$, where $\xi = \partial^2/(k_0^2 \partial z^2)$ and $\eta = n^2 - 1$. The parabolic equation (equation 21) is then expressed by:

$$\frac{\partial u}{\partial r} = \mathrm{i}k_0(\mathcal{P}'-1)u. \tag{24}$$

Assuming that the acoustic field exists at an arbitrary distance r_0 and, considering that $\mathcal{P}'$ slowly varies on the interval $[r_0, r_0+\Delta r]$, the solution of equation (23) is given by the expression

$$\begin{aligned} u(r_0, r_0+\Delta r) &= \exp[\mathrm{i}k_0(\mathcal{P}'-1)\Delta r]u(r_0, z) \\ &= \exp[s(\mathcal{P}'-1)]u(r_0, z). \end{aligned} \tag{25}$$

Assuming $\Im = \mathcal{P}'^2 - 1$, the idea is to approximate directly the exponential operator $\exp[s(\mathcal{P}'-1)]$. This can be carried out through a Padé development [49, 50].

In a first approach, when dealing with flat and homogeneous terrains, a second order Padé development [Padé (2,2)] has been used. In that case,

$$\begin{aligned} \exp\left[s(\mathcal{P}'-1)\right] &= \exp\left[s(\sqrt{1+\Im}-1)\right] \\ &\approx \frac{1 + p_1\Im + p_2\Im^2}{1 + q_1\Im + q_2\Im^2}. \end{aligned} \tag{26}$$

The coefficients p_1, p_2, q_1 and q_2 are easily deduced from a Taylor development of the exponential operator $\exp[s(\mathcal{P}'-1)]$. After identification, we obtain:

$$\begin{aligned} p_1 &= \frac{3+s}{4}, & p_2 &= \frac{s^2+6s+3}{48}, \\ q_1 &= \frac{3-s}{4}, & q_2 &= \frac{s^2-6s+3}{48}. \end{aligned} \tag{27}$$

When dealing with complex non-flat terrains, a first order Padé development [Padé (1,1)] is relevant enough to ensure good predicting results with an acceptable CPU time [51]. In that case, we obtain:

$$\exp\left[s(\mathcal{P}'-1)\right] = \exp\left[s(\sqrt{1+\Im}-1)\right] \approx \frac{1+p\Im}{1+q\Im}. \tag{28}$$

The coefficients p and q are respectively

$$p = \frac{1+s}{4}, \qquad q = \frac{1-s}{4}. \tag{29}$$

Comparison between the two Padé developments has been successfully performed. An example is shown in Figure 9.

Finally, the marching algorithm used to solve this problem is expressed in function of the coefficient and , and . For the Padé (2,2) development:

$$\begin{aligned} &\left[1 + q_1(\eta+\xi) + q_2(\eta+\xi)^2\right]u(r_0+\Delta r, z) \\ &= \left[1 + p_1(\eta+\xi) + p_2(\eta+\xi)^2\right]u(r_0, z), \end{aligned} \tag{30}$$

and for the Padé(1,1) development, respectively:

$$\begin{aligned} &\left[1 + q(\eta+\xi)\right]u(r_0+\Delta r, z) \\ &= \left[1 + p(\eta+\xi)\right]u(r_0, z). \end{aligned} \tag{31}$$

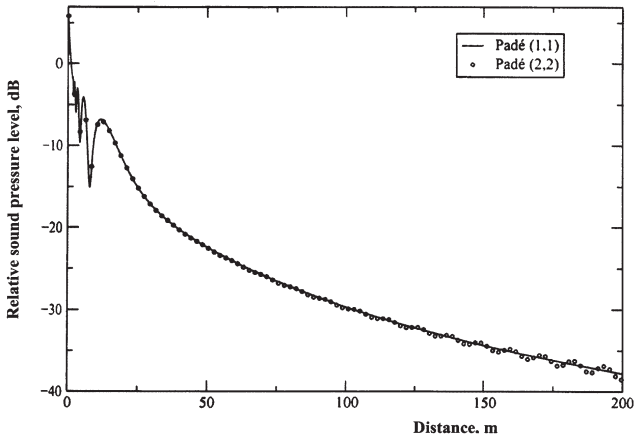

Figure 9. Comparison between Padé(2,2) and Padé(1,1) developments above a ground of finite impedance. Frequency: 500 Hz; $z_S = z_R = 2$ m; $\sigma = 200$ kN s m^{-4}.

In this approach, the ground is modelled as a local reacting surface with complex impedance, which may change along the sound wave path (case of mixed grounds). The mean vertical sound speed profiles are set constant along the distance and are logarithmically shaped as previously presented by Gilbert and White [42]:

$$c(z) = c_0 + a \ln \frac{z}{z_0}, \tag{32}$$

where z_0 is the roughness parameter and a the refraction parameter.

A non-reflecting boundary condition is imposed at the top of the computational domain by adding a very thick absorbing layer of several wavelengths. This can be assumed as equivalent to the Sommerfeld condition.

The starting field necessary to initialise the marching algorithm has a Gaussian shape, an adjustable width, and considers the image source weighed by a complex reflection coefficient.

The atmospheric turbulence is considered as isotropic, homogeneous and only due to temperature fluctuations. It is modelled by an averaging of N realisations of the refraction index, which random field is generated by a superposition of discrete random Fourier modes [52]. The turbulent energy spectrum depends on the choice of the turbulent spectrum, which profile is determined by the intensity $\langle\mu^2\rangle$ and the scale L already used in the analytical models (cf. section 2.2.2.). The Gaussian distribution and the von Karman turbulent spectrum are the most commonly used [53, 54]. The domain of the latter is wider, and thus, it better takes into account the turbulent eddies responsible for acoustic scattering in the atmosphere [52].

3.3. Validations in the case of sound propagation above a flat ground

Many validations were carried out for flat ground situations. Most of them are presented in [55]. Those validations were first performed with respect to other theoreti-

cal analytical and/or numerical models. In both cases, the agreement was particularly interesting.

As an example, let consider the complex situation involving sound wave propagation above a heterogeneous ground, through an acoustic shadow zone. In [22], the authors compared indoors experimental data obtained above a mixed ground with analytical prediction given by the residue series solution detailed in section 2.2.1. Those measurements were performed on a 1/10 scale-model. In order to simulate *in labo* the upward refraction, the surface was curved. The radius of curvature was 15 m. Assuming that the PE solution is only valid in the far field, we proceed to a scale change in order to correctly compare PE results with Bérengier and Daigle's data.

In Figure 10, the split-step Padé predictions provide a better fit than analytical solutions. According to the authors, this deviation beyond the impedance jump could be explained by the choice of the edge diffraction coefficient in the model, set to unity. After 25 m, the error is certainly amplified by the scale factor and by the strong linear gradient value due to the analogy between sound propagation above a curved surface in a homogeneous atmosphere and sound propagation in a stratified atmosphere above a plane surface [22].

In the configuration presented in Figure 10, no turbulence was considered. For larger distances more representative of real situations and, mainly for downward refraction conditions, turbulence that scatters sound energy in the shadow region has to be taken into account. Figure 11 shows the comparison between the Split-step Padé predictions, with and without turbulence, in the same propagation conditions as in Wiener and Keast experiments [56]. Without turbulence, the relative sound pressure level predictions rapidly decrease whereas turbulent predictions are very close to experimental data. Turbulent results are drawn for three different numbers of realizations, in order to give an idea of their convergence. The small discrepancy between predictions and measurements can be attributed to uncertainties in acoustic, climatic and ground impedance measurements. Nevertheless, the relative sound pressure level evolutions are very similar as far as turbulence is considered.

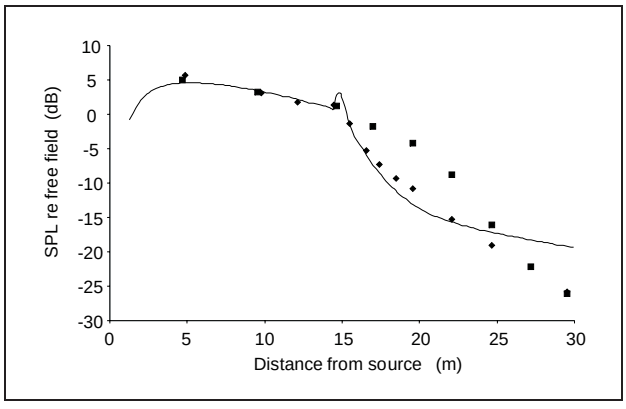

Figure 10. Mixed ground and upward refraction: Split-step Padé predictions (——) compared with experimental (◆◆◆) and theoretical (▪▪▪) results from [22]. Frequency = 400 Hz; $z_S = z_R = 0.5$ m; $\sigma_1 = 5 \cdot 10^4$ kN s m^{-4}; $\sigma_2 = 50$ kN s m^{-4}. Linear gradient until the altitude $z = 1.2$ m.

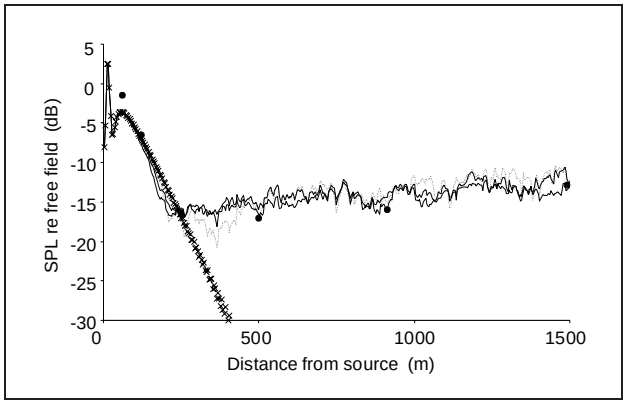

Figure 11. Split-step Padé predictions in deterministic (×) or turbulent cases (– – –: 10 realisations, ——: 20 realizations; ▬: 40 realisations) compared with experimental data (●) from Wiener and Keast [56]. Frequency = 424 Hz; $z_S = 1.2$ m; $z_R = 0.6$ m; $\sigma_1 = \sigma_2 = 200$ kN s m^{-4}; $a = -0.5$ m/s.

3.4. Validations in the case of sound propagation above a non-flat terrain

Several acoustic researchers have recently worked on the problem of the propagation above non-flat terrain. A curved terrain version of the parabolic equation has been adapted for acoustic propagation in the atmosphere over fairly simple terrain profiles, which can be reduced to a set of joined circular section pieces [57]. In this technique, a separate conformal coordinate transformation was applied to each circular section piece of atmosphere. Sack and West chose to use a transformation, which follows the terrain profile [46]. Their method is convenient for any smooth terrain but seems to be not adapted for a parabolic equation including wind terms. Thus, we chose to develop another model which can be used either above any kind of topography and with a parabolic equation including wind terms. The irregular ground is treated as a succession of flat domains as shown on Figure 12 [58, 59, 60].

Each flat domain in the coordinate system (r, z) is rotated so that the r-axis is always parallel to the ground. The calculation above each domain requires an initial solution. Then, the values of the initial solution for the domain $n + 1$ are obtained from the values of the pressure field of domain n, except for the first domain where a Gaussian starter is used. At the slope discontinuity between domain n and domain $n + 1$, the sound pressure continuity is insured along the following z-axis by the equation

$$u_{n+1} = u_n \exp(\mathrm{i}k_0 r_n). \tag{33}$$

Following the discretization of the whole terrain in several flat domains, the code has just to be applied for each of them after introduction of the adapted initial solution. The code can consider various impedance values in each domain.

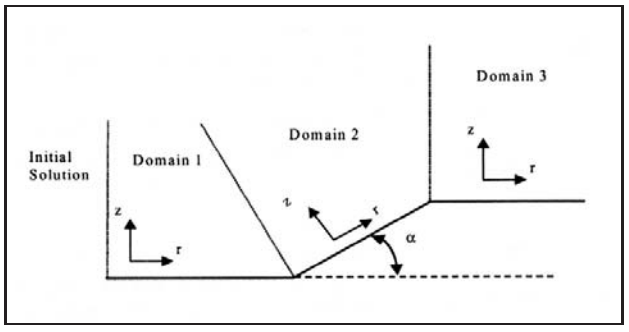

Figure 12. Complex topography: definition of the resolution domains.

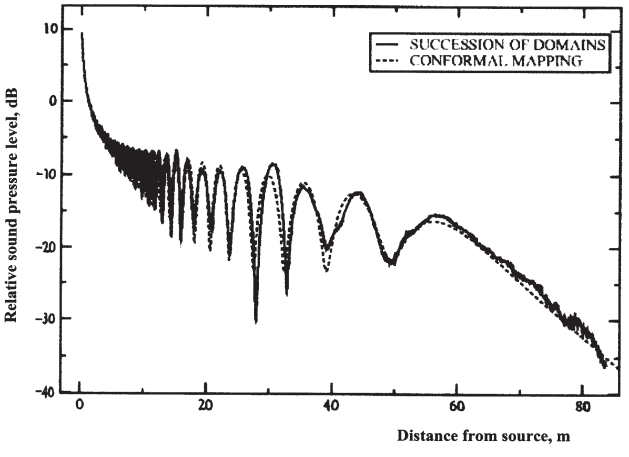

Figure 13. Relative sound pressure levels versus distance above a convex cylinder split in 8 flat domains. Frequency = 1000 Hz; $R_c = 100\,\mathrm{m}$; $z_S = z_R = 5\,\mathrm{m}$.

3.4.1. Validation above a theoretical non-flat surface

A first validation has been carried out on a theoretical non-flat surface. The propagation above a cylinder has been chosen as a benchmark case. The calculation can be also treated by a method using conformal mapping [57]. In the transformed domain where the ground is flat, the effect of topography is accounted for by an effective sound speed profile, which is exponentially increasing with height. For a convex cylinder, the sound speed profile used in the transformed domain is given by $c(z) = c_0 \exp(-z/R_c)$. R_c is the radius of curvature and c_0 the reference sound celerity. For this calculation performed for a frequency of 1000 Hz, the geometrical parameters are the following: $R_c = 100\,\mathrm{m}$, $z_s = 5\,\mathrm{m}$. The sound pressure is evaluated on a curved line at a constant height of 5 m above the cylinder. The curved surface is split in 8 flat domains; the angle between two flat domains is $\pi/32$ radians. On Figure 13, we plot the relative sound pressure level $20\log(p/p_{\mathrm{ref}})$, where p_{ref} is the sound pressure in front of the source at a distance of 1 m. The agreement between the two methods is very nice. Other comparisons have been carried out. The agreement is still good up to an angle of $\pi/16$ radians between the flat domains. Beyond this value, the approximation of the cylinder by flat domains gives rise to errors.

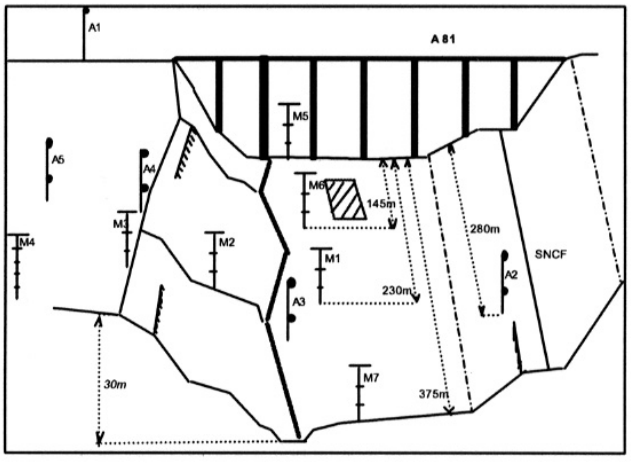

Figure 14. Schematic illustration of the site topography and the experimental set-up.

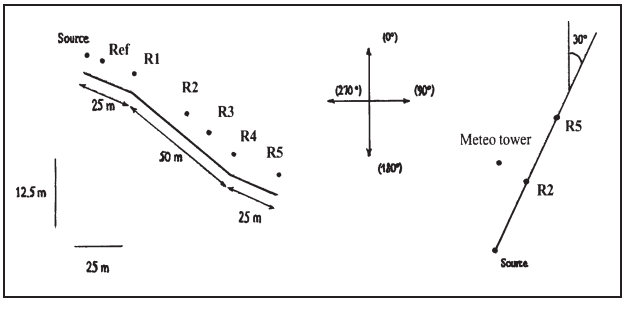

Figure 15. Experimental set-up.

3.4.2. Validation above a real non-flat terrain

An outdoor site near Saint-Berthevin (France) has been selected to study the influence of meteorological conditions on noise traffic. This offers the possibility to measure simultaneously, in various points of the site, detailed meteorological and noise propagation data for short periods as well as for a long-term monitoring. Figure 14 shows a schematic illustration of the site topography and the experimental set-up.

For a first comparison between experimental data measured on this complex site and the numerical PE simulations, we used an artificial broadband point source located 2 m above the ground and several receivers located at the same height as shown on Figure 15.

In the results presented on Figures 16 and 17, the direction of the mean wind was 20° North and the mean vertical velocity profile $u(z)$ was modelled using a logarithmic profile as mentioned in equation (31), with $a = 1.2$ and $z_0 = 0.1\,\mathrm{m}$. The characteristic impedance value of each domain of the ground surface has been determined according to the grazing incidence technique developed by Bérengier and Garai [17]. This measurement technique that requires a set of two microphones located 4 m away from an impulse source is similar to this already detailed in section 2.1.1. The estimation of the airflow resistivity value of the ground to be qualified is obtained through a Levenberg-Marquardt inverse fitting algorithm applied to

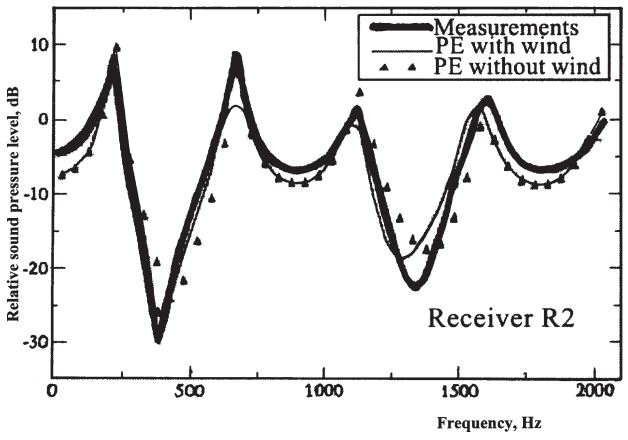

Figure 16. Complex topography: comparison between measured relative sound pressure level at receiver R2 and prediction using PE method: Influence of the mean wind. $d(S, R_2) = 50$ m, $\sigma_1(S, R_1) = 600$ kN s m^{-4}, $\sigma_2(R_1, R_2) = 90$ kN s m^{-4}.

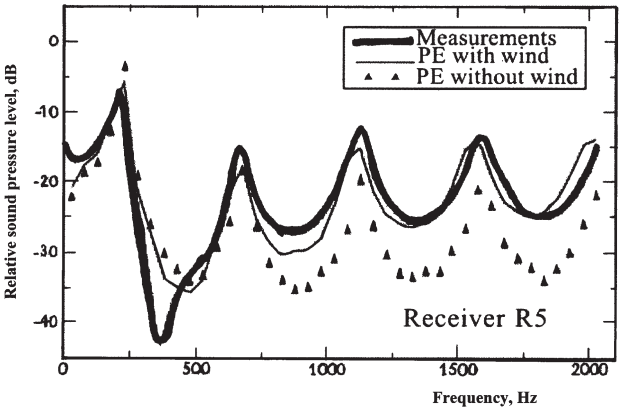

Figure 17. Complex topography: comparison between measured relative sound pressure level at receiver R5 and prediction using PE method: Influence of the mean wind. $d(S, R_5) = 50$ m, $\sigma_1(S, R_1) = 600$ kN s m^{-4}, $\sigma_2(R_1, R_5) = 90$ kN s m^{-4}.

the experimental narrow-band excess attenuation between the two microphones (cf. Figure 2). To run this procedure, we used the theoretical propagation model detailed in 2.1.1 (equation 1) and the Delany and Bazley impedance model [13]. This technique is very similar to the Nordic one developed by Ögren *et al.* [61], which is based on a 1/3 octave analysis of measurement data carried out at four levels instead of one in our method. The following values of the airflow resistivity have been found: between the source and receiver R1, $\sigma = 600$ kN s m^{-4} and from R1 to R5, $\sigma = 90$ kN s m^{-4}.

The distances of propagation are respectively 25 m between the source and R1 and 75 m from R1 to R5. A reference microphone is located 10 m from the source at 2 m above the ground.

As shown on Figure 16, at a short distance (Receiver R2), wind influence is small. In the other hand, for larger distance, for instance at the receiver R5 placed down the hill, we clearly observe the wind influence (see Figure 17). In that case, if the mean wind profile is not taken into account in the numerical simulation, large differences between prediction and measured data are identified up to 500 Hz. The difference is of the order of 15 dB. When the mean velocity profile is introduced into the PE simulation, the agreement between computed and measured values becomes reasonable. The remaining discrepancies could be attributed to the variations of the local impedance and to the fluctuations of the meteorological parameters: mainly, mean wind direction and turbulence intensity and scale. Concerning the back-scattered sound energy by slopes, N. Blairon [51] showed that the ratio between the scattered and the total acoustic energy is less than 0.1% for a frequency of 500 Hz and a slope of 40 degrees.

4. Conclusion

During the years 1970–1980, the large increase of noisy transportation means and industrial sites required to improve the different predicting methods concerning long range sound propagation outdoors and particularly by introducing ground effects and later, the influence of the meteorological conditions.

During this period, the evolution of the techniques allowed to improve the theoretical models in order to be as close as possible of real situations. So, the influences of discontinuous grounds and atmospheric conditions have successively been considered.

As the analytical approaches mainly based on the geometrical acoustics are relevant for simple situations, they become rapidly inadequate for complex sites. In that case, numerical methods have to be implemented. Results presented in this paper seem for all the techniques very promising, and particularly the numerical PE approach, which is now able to consider both complex topographies and meteorological conditions.

Therefore, researches on this very important field are always progressing. New developments have recently been published during the 10th Long Range Sound Propagation Symposium in 2002. They deal with a hybrid method using in the near field a BEM technique and the parabolic approach in the far field [62, 63]. Other techniques can also be implemented; for instance, those based on the linearized Eulerian model [64]. The large improvements observed in the last decade were only possible thanks to the close collaboration between researchers involved in outdoor acoustics and meteorology of the low atmosphere layers [65].

At the beginning, the main goal was only the characterisation of the acoustic field in a half space above grounds. Further, the various results obtained in the recent years have been used for standardisation and national regulation. One of the main French applications concerns the elaboration of the national predicting method for traffic noise [30], which certainly would not be issued without the important contribution of fundamental researches on the modelling of the various propagation phenomena.

Currently, the main work is to study over long time periods the statistical effects of meteorology on outdoor sound

propagation in order to rapidly answer to the European regulations elaborated in the framework of the new noise directive [66].

References

[1] K. Attenborough, S. I. Hayek, J. M. Lawther: Propagation of sound above a porous half space. J. Acoust. Soc. Am. **68** (1980) 1493–1501.

[2] M. Bérengier, M. Stinson, G. Daigle, J. F. Hamet: Porous road pavements: Acoustical characterization and propagation effects. J. Acoust. Soc. Am. **101** (1997) 155–162.

[3] G. A. Daigle, M. R. Stinson, D. I. Havelock: Experiments on surface waves over a model impedance plane using acoustic pulses. J. Acoust. Soc. Am. **99** (1996) 1993–2005.

[4] I. Rudnick: The propagation of an acoustic wave along a boundary. J. Acoust. Soc. Am. **19** (1947) 348–356.

[5] R. Donato: Propagation of a spherical wave near a plane boundary with complex impedance. J. Acoust. Soc. Am. **60** (1976) 34–39.

[6] C. I. Chessell: Propagation of noise along a finite impedance boundary. J. Acoust. Soc. Am. **62** (1977) 825–834.

[7] T. F. W. Embleton, J. E. Piercy, N. Olson: Outdoor sound propagation over a ground of finite impedance. J. Acoust. Soc. Am. **59** (1976) 267–277.

[8] T. F. W. Embleton, J. E. Piercy, G. A. Daigle: Effective flow resistivity of ground surfaces determined by acoustical measurements. J. Acoust. Soc. Am. **74** (1983) 1239–1244.

[9] S. I. Thomasson: Reflection of waves from a point source by an impedance boundary. J. Acoust. Soc. Am. **59** (1976) 780–785.

[10] S. I. Thomasson: A powerful asymptotic solution for sound propagation above an impedance boundary. Acustica **45** (1980) 122–125.

[11] D. Habault, P. J. T. Filippi: Ground effect analysis: Surface wave and layer potential representations. J. Sound and Vib. **79** (1981) 529–550.

[12] D. Habault: Etude de l'influence des sols sur la propagation sonore. Ph.D. thesis, Université Aix-Marseille I, Marseille, 1984.

[13] M. E. Delany, E. N. Bazley: Acoustical properties of fibrous absorbent materials. Applied Acoustics **3** (1970) 105–116.

[14] J. F. Hamet, M. Bérengier: Acoustical characteristics of porous pavements: A new phenomenological model. Internoise '93, Leuven, Belgium, 1993, 641–646.

[15] K. Attenborough, C. Howorth: Models for the acoustic characteristics of porous road surfaces. Int. Tire/Road Noise Conf., Gothenburg, Sweden, 1990, 177–191.

[16] Y. Champoux, M. R. Stinson: On acoustical models for sound propagation in rigid frame porous materials and the influence of shape factors. J. Acoust. Soc. Am. **92** (1992) 1120–1131.

[17] M. Bérengier, M. Garai: A state-of-the-art of in situ measurement of the sound absorption coefficient of road pavements. 11th International Congress on Acoustics, Rome, Italy, 2001, Volume II, CD–Rom ISBN 88–88387.

[18] K. B. Rasmussen: A note on the calculation of sound propagation over impedance jumps and screens. J. Sound and Vib. **84** (1982) 598–602.

[19] B. de Jong, A. Moerkerken, J. D. van der Toorn: Propagation of sound over grassland and over earth barrier. J. Sound and Vib. **86** (1983) 23–46.

[20] P. Koers: Diffraction by an absorbing barrier or by an impedance transition. Internoise'83, 1983, 311–314.

[21] V. Zouboff, Y. Brunet, M. Bérengier, E. Séchet: A qualitative approach of atmospheric effects on long range sound propagation. 6th Int. Symp. on Long Range Sound Propagation, Ottawa, Canada, 1994, 251–269.

[22] M. Bérengier, G. Daigle: Diffraction of sound above a curved surface having an impedance discontinuity. J. Acoust. Soc. Am. **84** (1988) 1055–1060.

[23] J. Defrance: Méthode analytique pour le calcul de propagation du bruit extérieur. Ph.D. thesis, Université du Maine, Le Mans, France, 1996.

[24] A. D. Pierce: Acoustics: an introduction to its physical principles and application. Mc Graw-Hill, New York, 1981. chapter 9.

[25] D. A. Hill, J. R. Wait: HF ground wave propagation over mixed land, sea and sea-ice paths. IEEE Trans. Geosci. Rem. Sens, GE **19** (1981) 210–216.

[26] R. M. Jones: How edge diffraction couples ground wave modes at a shoreline. Radio science **19** (1984) 959–965.

[27] T. Hidaka, K. Kageyama, S. Masuda: Sound propagation in the rest atmosphere with linear sound velocity profile. J. Acoust. Soc. Japan (E) **6** (1985) 117–125.

[28] A. L'Espérance, P. Herzog, G. A. Daigle, J. R. Nicolas: Heuristic model for outdoor sound propagation based on an extension of the geometrical ray theory in the case of a linear sound speed profile. Applied Acoustics **37** (1992) 111–119.

[29] M. Bérengier: Approche probabiliste de la propagation du bruit en milieu extérieur. Thème de recherche EGU 03: Synthèse finale, LCPC Report, 1996.

[30] CERTU, SETRA, LCPC, CSTB: Bruit des infrastructures routières: Méthode de calcul incluant les effets météorologiques. version expérimentale. NMPB – Routes – 96, 1997.

[31] AFNOR XPS 31 133 Standard: Acoustique - Bruit des infrastructures de transports terrestres - Calcul de l'atténuation du son lors de sa propagation en milieu extérieur, incluant les effets météorologiques. AFNOR, Paris, 2001.

[32] ISO 9613-1 Standard: Acoustics - attenuation of sound during propagation outdoors – Part 1: Calculation of the absorption of sound by the atmosphere. International Standard Organisation, Geneva, 1993.

[33] G. A. Daigle: Effects of atmospheric turbulence on the interference of sound waves above a finite impedance boundary. J. Acoust. Soc. Am. **65** (1979) 45–49.

[34] R. Raspet, S. W. Lee, E. Kuester, D. C. Chang, W. F. Richards, R. Gilbert, N. Bong: A fast-field program for sound propagation in a layered atmosphere above an impedance ground. J. Acoust. Soc. Am. **77** (1985) 345–352.

[35] R. Raspet, W. Wu: Calculation of average turbulence effects on sound propagation based on the fastfield program formulation. J. Acoust. Soc. Am. **97** (1995) 147–153.

[36] S. N. Chandler-Wilde, D. C. Hothersall: Sound propagation above an inhomogeneous impedance plane. J. Sound and Vib. **98** (1985) 475–491.

[37] S. N. Chandler-Wilde, D. C. Hothersall: Efficient calculation of the green function for acoustic propagation above a homogeneous impedance plane. J. Sound and Vib. **180** (1995) 705–724.

[38] F. Anfosso-Lédée, P. Dangla: Modélisation numérique du fonctionnement des écrans antibruit routiers dans leur en-

vironnement. Bull. des Laboratoires des Ponts et Chaussées **203** (1996) 45–54.
[39] P. Boulanger, T. Waters-Fuller, K. Attenborough, K. M. Li: Models and measurements of sound propagation from a point source over mixed impedance ground. J. Acoust. Soc. Am. **102** (1997) 1432–1442.
[40] E. Premat, Y. Gabillet: A new boundary-element method for predicting outdoor sound propagation and application to the case of sound barrier in the presence of downward refraction. J. Acoust. Soc. Am. **108** (2000) 2775–2783.
[41] F. D. Tappert, R. H. Hardin: Computer simulation of long range oceanic acoustic propagation using the parabolic equation method. 8th Int. Congress on Acoustics, London, UK, 1974, 452.
[42] K. E. Gilbert, M. J. White: Application of the parabolic equation to sound propagation in a refracting atmosphere. J. Acoust. Soc. Am. **85** (1989) 630–637.
[43] J. M. Craddock, M. J. White: Sound propagation over a surface with varying impedance: A parabolic equation approach. J. Acoust. Soc. Am. **91** (1992) 3184–3191.
[44] X. Di, K. E. Gilbert: Application of a fast Green's function method to long range sound propagation in the atmosphere. 5th Int. Symp. on Long Range Sound Propagation, Milton Keynes, UK, 1992, 128–141.
[45] E. M. Salomons: Improved Green's function parabolic equation method for atmospheric sound propagation. J. Acoust. Soc. Am. **104** (1998) 100–111.
[46] R. A. Sack, M. West: A parabolic equation for sound propagation in two dimensions over any smooth terrain profile: the generalized terrain parabolic equation (gt-pe). Applied Acoustics **45** (1995) 113–129.
[47] L. Dallois, P. Blanc-Benon, D. Juvé: A wide-angle parabolic equation for acoustic waves in inhomogeneous media: Applications to atmospheric sound propagation. J. Comp. Acoust. **9** (2001) 477–494.
[48] P. Blanc-Benon, L. Dallois, D. Juvé: Long range sound propagation in a turbulent atmosphere within the parabolic approximation. Acta Acustica united with Acustica **87** (2001) 659–669.
[49] M. D. Collins: A split-step Padé solution for the parabolic equation method. J. Acoust. Soc. Am. **93** (1993) 1736–1742.
[50] P. Chevret, P. Blanc-Benon, D. Juvé: A numerical model for sound propagation through a turbulent atmosphere near the ground. J. Acoust. Soc. Am. **100** (1996) 3587–3599.
[51] N. Blairon: Effet de la topographie sur la propagation des ondes acoustiques dans l'atmosphère: modélisation avec l'équation parabolique et validation sur un site extérieur. PhD thesis, Ecole Centrale de Lyon, 2002.
[52] D. Juvé, P. Blanc-Benon, P. Chevret: Numerical solutions of sound propagation through a turbulent atmosphere. 5th Int. Symp. on Long Range Sound Propagation, Milton Keynes, UK, 1992, 282–296.
[53] G. A. Daigle, J. E. Piercy, T. F. W. Embleton: Line-of-sight propagation through atmospheric turbulence near the ground. J. Acoust. Soc. Am. **74** (1983) 1505–1513.
[54] A. Ishimaru: Wave propagation and scattering in random media. Academic, New-York, 1978. vol.2.
[55] B. Gauvreau, M. Bérengier, P. Blanc-Benon, C. Depollier: Traffic noise prediction with the parabolic equation method: Validation of a split-step Padé approach in complex environments. J. Acoust. Soc. Am. **112** (2002) 2680–2687.
[56] F. M. Wiener, D. N. Keast: Experimental study of the propagation of sound over ground. J. Acoust. Soc. Am. **31** (1959) 724–733.
[57] X. Di, K. E. Gilbert: The effect of turbulence and irregular terrain on outdoor sound propagation. 6th Int. Symp. on Long Range Sound Propagation, Ottawa, Canada, 1994, 315–333.
[58] N. Blairon, P. Blanc-Benon: Propagation d'une onde acoustique au dessus d'un sol non plan: utilisation de l'équation parabolique. 15th Congrès Français de Mécanique, Nancy, France, 2001, CD Rom.
[59] N. Blairon, P. Blanc-Benon, M. Bérengier, D. Juvé: Calculation of sound propagation over non flat terrain using parabolic equation. 11th Int. Congress on Acoustics, Rome, Italy, 2001, Volume III, CD–Rom ISBN 88–88387–02–01.
[60] N. Blairon, P. Blanc-Benon, M. Bérengier, D. Juvé: Outdoor sound propagation in complex environments: experimental validation of a pe approach. 10th Int. Symp. on Long Range Sound Propagation,, Grenoble, France, 2002.
[61] M. Ögren, H. Jonasson: Measurement of the acoustic impedance of ground. Nordtest Project 1365-1997. SP Report 1998:28, Boras, Sweden, 1999.
[62] I. N. Noordhoek, E. M. Salomons: Coupling of PE with BEM or with a ray model for the evaluation of complex noise barriers in a refracting atmosphere. 10th Int. Symp. on Long Range Sound Propagation, Grenoble, France, 2002.
[63] E. Premat, J. Defrance, M. Priour, F. Aballéa: A hybrid GFPE-BEM approach for complex outdoor sound propagation. 10th Int. Symp. on Long Range Sound Propagation, Grenoble, France, 2002.
[64] R. Blumrich, D. Heimann: A linearized eulerian sound propagation model for studies of complex meteorological effects. J. Acoust. Soc. Am. **102** (1997) 446–455.
[65] R. B. Stull: An introduction to boundary layer meteorology. Kluwer Academic, Dordrecht, The Netherlands, 1988.
[66] Directive of the European parliament and of the council relating to the assessment and management of environmental noise. 25 June 2002.